Sustainable Energy & Fuels

Intercalative and non-intercalative photo-recharge using all-solid-state cells for solar energy conversion and storage

Journal:	*Sustainable Energy & Fuels*
Manuscript ID	SE-ART-12-2023-001636.R1
Article Type:	Paper
Date Submitted by the Author:	06-Feb-2024
Complete List of Authors:	Yoshimoto, Masataka; Tokyo Institute of Technology School of Materials and Chemical Technology Department of Chemical Science and Engineering Tamura, Kazuhisa; Japan Atomic Energy Agency, Materials Sciences Research Center Watanabe, Kenta; Tokyo Institute of Technology School of Materials and Chemical Technology, Department of Chemical Science and Engineering Shimizu, Keisuke; Tokyo Institute of Technology Institute of Innovative Research, Research Center for All-Solid-State Battery Kobayashi, Takeshi; Tokyo Institute of Technology, Interdisciplinary Graduate School of Science and Engineering, Department of Electronic Chemistry Tsurita, Hanae; Tokyo Institute of Technology, Interdisciplinary Graduate School of Science and Engineering, Department of Electronic Chemistry Horisawa, Yuhei; Tokyo Institute of Technology School of Materials and Chemical Technology Department of Chemical Science and Engineering Suzuki, Kota; Tokyo Institute of Technology Institute of Innovative Research, Research Center for All-Solid-State Battery Kanno, Ryoji; Tokyo Institute of Technology Institute of Innovative Research, Research Center for All-Solid-State Battery Hirayama, Masaaki; Tokyo Institute of Technology School of Materials and Chemical Technology Department of Chemical Science and Engineering; Tokyo Institute of Technology Institute of Innovative Research, Research Center for All-Solid-State Battery

ARTICLE

Intercalative and non-intercalative photo-recharge using all-solid-state cells for solar energy conversion and storage

Received 00th January 20xx,
Accepted 00th January 20xx

DOI: 10.1039/x0xx00000x

Masataka Yoshimoto,[a] Kazuhisa Tamura,[b] Kenta Watanabe,[a*] Keisuke Shimizu,[c] Yuhei Horisawa,[a] Takeshi Kobayashi,[d] Hanae Tsurita,[d] Kota Suzuki,[c] Ryoji Kanno[c] and Masaaki Hirayama[a,c*]

Photo-rechargeable systems, which can efficiently convert and store solar energy into chemical energy within single devices, are essential to harness sunlight effectively. Photo-(de)intercalation plays a pivotal role in the functionality of photo-rechargeable systems. Nevertheless, the photo-(de)intercalation process has not been conclusively confirmed owing to potential interference from side reactions, such as the decomposition of liquid electrolytes and the elution of electrode materials. In this study, we successfully demonstrated photo-responsive Li^+-deintercalation using an all-solid-state thin-film battery comprised of epitaxially-grown anatase TiO_2 doped with Nb (a-TiO_2:Nb) as the cathode, in combination with *operando* X-ray diffractometry. Under light irradiation, Li^+-deintercalation occurred and was subsequently reversibly intercalated into a-TiO_2:Nb during discharge. Furthermore, it was observed that a portion of the charge capacity under light irradiation resulted from non-intercalative (non-redox-reactive) electron transfer, akin to supercapacitors. These findings suggest that both intercalative and non-intercalative photo-charging mechanisms can be applied to secondary batteries and supercapacitors, respectively. Therefore, photo-rechargeable all-solid-state cells, encompassing both secondary batteries and supercapacitors, hold significant promise for advancing solar energy conversion and storage.

Introduction

Solar energy has garnered considerable attention as a renewable energy source, addressing energy, environmental, and resource-related concerns.[1–8] A critical challenge in using solar energy is ensuring a steady supply. Renewable energy sources are inherently intermittent owing to weather changes and seasonal variations, making continuous provision challenging. Solar energy, despite its merits, shares this limitation. Consequently, achieving a reliable supply of solar energy as electrical power necessitates both effective conversion and efficient storage capabilities.

Solar cells are exemplary devices for converting solar energy, yet they do not possess the ability to store the energy they produce. Recently, photocatalytic water splitting has gained prominence as a solar energy conversion system capable of converting solar energy into hydrogen, a form of chemical energy that can be stored. However, the safe storage and large-scale transportation of hydrogen pose significant challenges. The overall system cost is likely high because the storage component is separate from the conversion unit. Hence, there is a pressing need for innovative devices that integrate both conversion and storage functionalities to facilitate the practical utilization of solar energy. Some reports have highlighted devices that can achieve both these functions within a single unit, such as photocapacitors[9,10] and energy-storable dye-sensitised solar cells.[11] However, photocapacitors exhibit a disadvantage in the form of a linear decrease in discharge voltage, making them less suitable for prolonged continuous usage. On the other hand, energy-storable dye-sensitised solar cells consist of distinct conversion and storage components, strictly adhering to a segregated design. Therefore, developing an alternative device that seamlessly combines solar energy conversion and storage capabilities is paramount.

A photo-(de)intercalative rechargeable battery (PIRB) is an ideal device combining conversion and storage functionalities. Conventional Li-ion batteries rely on Li^+-(de)intercalation driven by external bias, whereas PIRBs harness photovoltages generated within the electrodes to facilitate Li^+-(de)intercalation. Consequently, the electrodes must be responsive to incident light, triggering a redox reaction concomitant with Li^+-(de)intercalation. The generation of photovoltage occurs through the photoexcitation of electrons from the valence band (VB) to the conduction band (CB) within a semiconductor, typically aligning with its band gap (BG). As such, semiconductor materials are employed as electrodes to facilitate photo-(de)intercalation. Notably, Tributsch reported the concept of photo-intercalation using semiconductor

[a] *Department of Chemical Science and Engineering, School of Materials and Chemical Technology, Tokyo Institute of Technology, 4259 Nagatsuta-cho, Midori-ku, Yokohama 226-8501, Japan. Email: watanabe.k.cy@m.titech.ac.jp, hirayama@mac.titech.ac.jp*
[b] *Materials Sciences Research Center, Japan Atomic Energy Agency, 1-1-1, Koto, Sayo, Hyogo 679-5148, Japan.*
[c] *Research Center for All-Solid-State Battery, Institute of Innovative Research, Tokyo Institute of Technology, 4259 Nagatsuta-cho, Midori-ku, Yokohama 226-8501, Japan.*
[d] *Department of Electronic Chemistry, Interdisciplinary Graduate School of Science and Engineering, Tokyo Institute of Technology, 4259 Nagatsuta-cho, Midori-ku, Yokohama 226-8501, Japan.*
Electronic Supplementary Information (ESI) available. See DOI: 10.1039/x0xx00000x

materials as electrodes back in 1980.[12,13] Recently, TiO_2 and WO_3 as electrodes for photo-(de)intercalation has been documented.[14–20] In the context where the host and guest materials are MO_2, representing an n-type semiconductor, and Li^+ ions, respectively, the charge transfer under photo-irradiation is expected to proceed via the following reactions (1)~(5).

$$x\mathrm{h}\nu \rightarrow x\mathrm{e}^- + x\mathrm{h}^+ \quad \text{(in cathode)} \quad (1)$$

$$\mathrm{Li}_x\mathrm{M}^{3+}{}_x\mathrm{M}^{4+}{}_{1-x}\mathrm{O}_2 + \mathrm{h}^+ \rightarrow \mathrm{M}^{4+}\mathrm{O}_2 + x\mathrm{Li}^+ \quad \text{(at cathode/positive electrode)} \quad (2)$$

$$x\mathrm{e}^- \text{ (cathode)} \rightarrow x\mathrm{e}^- \text{ (anode)} \quad \text{(via external circuit)} \quad (3)$$

$$x\mathrm{Li}^+ \text{ (cathode)} \rightarrow x\mathrm{Li}^+ \text{ (anode)} \quad \text{(via electrolyte)} \quad (4)$$

$$x\mathrm{Li}^+ + x\mathrm{e}^- \rightarrow x\mathrm{Li}^0 \quad \text{(at anode/negative electrode)} \quad (5)$$

When Li_xMO_2 (cathode) is exposed to light with energy levels exceeding its BG, electrons are excited from CB to VB, generating holes in the VB (1). These photogenerated holes subsequently facilitate the oxidation of M^{3+} to M^{4+}, initiating the deintercalation of Li^+ for the charge compensation (2). Photoexcited electrons migrate towards the counter electrode (anode) through the external circuit (3), while concurrently, Li^+ ions deintercalate from the Li_xMO_2 and move towards the counter electrode via the electrolyte (4). Ultimately, electrons originating from the Li_xMO_2 electrode reduce Li^+ ions to Li^0 at the counter electrode (5). However, the photo-(de)intercalation process has not been conclusively confirmed. This is primarily due to the inherent difficulty in isolating the currents attributed to photo-(de)intercalation from those resulting from side reactions, such as the decomposition of electrolytes and the dissolution of electrodes. Furthermore, these side reactions contribute to the instability of PIRBs, primarily because of the liquid nature of the electrolytes. Additionally, the photovoltages tend to accelerate these side reactions. Consequently, PIRBs must be durable to photovoltages and inactive to side reactions.

All-solid-state batteries (ASSBs) that employ solid electrolytes are particularly well-suited for PIRBs. The use of solid electrolytes effectively mitigates the dissolution of electrode materials. Furthermore, the durability of photovoltages is enhanced when employing solid electrolytes, as observed potential windows (≥ 5 V) of solid electrolytes typically exceed those of liquid electrolytes (≤ 4.6 V).[21–24] Moreover, the transference numbers of charge carriers in solid electrolytes are nearly 1, as other constituent elements are immobilised within crystal lattices. As a result, side reactions are effectively suppressed, even at the interfaces between electrodes and solid electrolytes, allowing for continuous operation. We have previously reported the stable photoelectrochemical reaction in an all-solid-state cell employing anatase TiO_2 doped with Nb (a-TiO_2:Nb) as the photo-responsive electrode, amorphous Li_3PO_4 (LPO) as the solid electrolyte, and metallic Li as the counter electrode.[25]. Nevertheless, the precise nature of the photoelectrochemical reactions in this context has not yet been fully elucidated.

In the context of all-solid-state cells, photo-responsive materials that do not undergo (de)intercalation processes could potentially find applications as electrodes in photo-rechargeable supercapacitors. This is because side reactions originating from electrolytes can be eliminated in such systems. When semiconductor electrodes are exposed to light with energy levels exceeding their BG, photovoltage, photo-excited electrons, and holes are generated. If these photogenerated electrons and holes can be effectively separated and directed to two distinct electrodes within a cell, using the photovoltage without engaging in electrochemical reactions, it becomes possible to charge the cell as if it were a supercapacitor utilizing photo energy. Thus, it is vital to ascertain whether the process of photo-charging is intercalative or non-intercalative.

Operando X-ray diffractometry (XRD) represents a valuable technique for investigating changes in the crystal structures of electrode materials during charge and discharge processes.[26] Epitaxially-grown electrode films are particularly well-suited for analysis using *operando* XRD, as each crystal facet can be individually examined. We have elucidated the principles underlying charge and discharge through analyses of epitaxially-grown electrode films employing *operando* XRD.[27–30] Thus, it is anticipated that intercalative and non-intercalative photo-charging can be investigated effectively by employing epitaxially-grown films in conjunction with *operando* XRD.

In this study, an epitaxial film of a-TiO_2:Nb was grown to serve as both the photo-responsive and Li^+-(de)intercalative electrode. The a-TiO_2:Nb epitaxial film was subjected to *operando* XRD measurements during charge and discharge processes to verify whether Li^+ ions were deintercalated from the a-TiO_2:Nb material when exposed to irradiated light.

Experimental

Sample preparation

The epitaxial a-TiO_2:Nb film was fabricated using a pulsed laser deposition (PLD) system (PSAD-3000 and PLAD-312, AOV Inc.), which consisted of a KrF excimer laser (COMPex201, Lambda Physik/Coherent) operating at a wavelength of 248 nm. Initially, a $CaRuO_3$ film was epitaxially deposited as a current collector onto a $LaSrAlO_4$(001) single-crystal substrate (10×10×0.5 mm^3, Crystal Base Co., Ltd.). Subsequently, the a-TiO_2:Nb film was epitaxially stacked on the $CaRuO_3$ layer. The PLD process utilised $CaRuO_3$ and $Ti_{0.95}Nb_{0.05}O_2$ (Toshima Manufacturing Co., Ltd.) as the target materials. The actual amount of doped Nb in the fabricated film was about 3 mol%. For battery performance, the doping level of Nb in a-TiO_2 should be increased from the viewpoint of the electronic conductivity.[31] However, for high photocatalytic activities, doping levels tend to be up to 2 mol%.[32-35] Therefore, the doping level of Nb was set to be about 3% to ensure both electronic conductivity and photoresponsivity in the present study.

A radio frequency (RF) magnetron sputtering system (PSAD-3000, AOV Inc.) was employed to synthesise the LPO solid electrolyte film. An LPO pellet (ϕ 50 mm × 4 mm thickness, Toshima Manufacturing Co., Ltd.) served as the target material

under the following conditions: target-to-substrate distance of 90 mm, pressure of 0.5 Pa in an argon atmosphere, substrate temperature of approximately 300 K, RF power set at 100 W, and a deposition time of 12 h.

Finally, a metallic Li film was deposited atop the Li_3PO_4 layer using the vacuum vapour deposition method (E-80Li, ALS Technology IncE-80Li) under the following conditions: target-to-substrate distance of 230 mm, chamber pressure maintained below 5.0×10^{-4} Pa, substrate temperature approximately 300 K, current set at 50 A, voltage at 1 V, and deposition duration of 0.5 h. It is worth noting that all these processes were conducted in an inert atmosphere to prevent the synthesised films from reacting with moisture present in the air.

Characterisation

The crystal orientations of the thin films were characterised using XRD with Cu Kα1 radiation (ATX-G and Smartlab, Rigaku Co., Ltd.). The thickness, density, and roughness of the films were determined by X-ray reflectivity (XRR) using the same diffractometers as XRD measurements. The obtained XRR spectra were analysed using the Parratt32 program.[36] The thickness of the films was also determined by thin-film stylus profilometry (DektakXT, Bruker Inc.).

(Photo)electrochemical measurements

Photoelectrochemical measurements of the batteries were conducted within a shielded enclosure (Probeh-toy-2, Toyo Technica Co., Ltd.) located within an argon-filled glove box to prevent any unwanted reactions with moisture from the ambient air. Charge and discharge measurements were carried out using multi-channel potentiostats/galvanostats (VSP300 and SP-200, Bio-logic Co.) with a current range of 0.1-0.5 C, voltage range of 0.75-4.5 V and operated in constant-current + constant-voltage (CC-CV) mode. A light-emitting diode (LED) with a central wavelength of 365 nm (LED365-SPT, Optocode Co., Ltd.) served as the light source. The distance between the light source and the batteries was maintained at 10 cm, sufficient to minimise thermal effects. Further details regarding the measurement setup and conditions can be found in Fig. S1 and S2.

Operando XRD measurements

Operando XRD measurements during (photo)charge/discharge were conducted to monitor structural changes in a-TiO_2:Nb films. These measurements were carried out using a κ-type six-circle diffractometer (Newport Corporation, USA) and a 6-Circle diffractometer (HUBER Diffraktionstechnik GmbH & Co. KG, Germany), which were installed at the beamlines BL14B1, BL22XU, and BL46XU at the SPring-8 synchrotron facility in Japan. The X-rays were monochromatised using a Si(111) double-crystal system, with an X-ray wavelength of 0.82518 Å (15 keV) employed. To prevent deactivation of the Li anode, the XRD measurements were conducted under vacuum conditions, following the methodology described in our prior work using an exclusive cell.[30] The charge/discharge measurements were performed with a current range of 0.1 C, voltage range of 0.75-4.5 V, and in CC-CV mode. A small LED with a central wavelength of 365 nm (OSV1YL5111A, OptoSupply) was used as the light source for the *operando* measurement.

Results and discussion

Fabrication of a-TiO_2:Nb epitaxial film as the cathode of the photo-rechargeable battery

First, the acquired a-TiO_2:Nb film underwent characterisation through various techniques, including XRD, XRR, DRS, and electrochemical tests under dark conditions. Fig. 1 illustrates the XRD pattern of the a-TiO_2:Nb film deposited using the PLD method on a $CaRuO_3$/$LaSrAlO_4$(001) substrate. The XRD pattern was recorded in the out-of-plane direction, and the discernible peaks, distinct from the $LaSrAlO_4$(001) substrate, were identified as the reflections from $CaRuO_3$ 001, $CaRuO_3$ 002 and a-TiO_2:Nb 004. In the in-plane direction (as shown in Fig. S3), the peaks attributed to a-TiO_2:Nb could not be unequivocally confirmed due to their overlap with the $LaSrAlO_4$-derived peaks. This overlap arises from the closely matching lattice constants 'a' and 'b' of a-TiO_2:Nb with those of $LaSrAlO_4$. Paradoxically, the non-confirmation of peaks in the in-plane XRD pattern implies that the ab planes of a-TiO_2:Nb are aligned with those of the $LaSrAlO_4$ substrate. Consequently, it can be deduced that a-TiO_2:Nb was epitaxially grown on $CaRuO_3$. The thickness and surface roughness of a-TiO_2:Nb/$CaRuO_3$/$LaSrAlO_4$(001) were further assessed using XRR, as depicted in Fig. S4. The fitting parameters are summarised in Table S1. The thickness of a-TiO_2:Nb was determined to be 10.7 nm. Hence, the entire a-TiO_2:Nb layer can absorb incident light, as film-type photoelectrodes thicker than 100 nm can transmit incident light in tandem-type photoelectrochemical cells.[37-40] The surface roughness of a-TiO_2:Nb measured at 0.3 nm suggests a remarkably smooth surface that minimises light scattering. This property renders the a-TiO_2:Nb film surface well-suited for efficient light absorption. The XRD and XRR findings affirm the successful fabrication of the epitaxial a-TiO_2:Nb film, characterised by its sufficient thinness and smooth surface.

Additionally, the absorption spectrum of a-TiO_2:Nb/$LaSrAlO_4$(001) indicates that the a-TiO_2:Nb film can

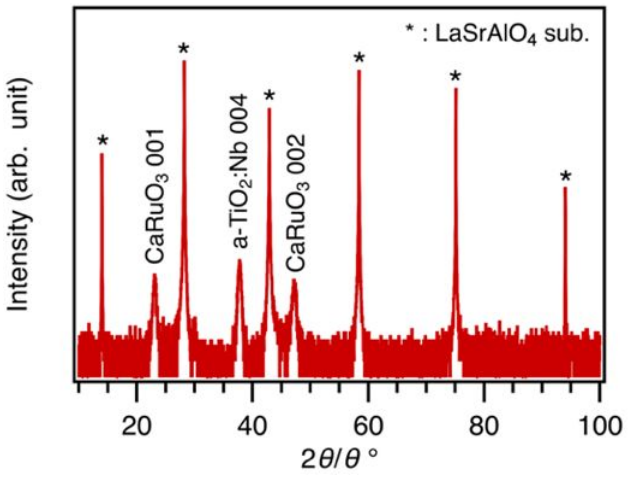

Fig. 1 An X-ray diffraction pattern at out-of-plane direction.

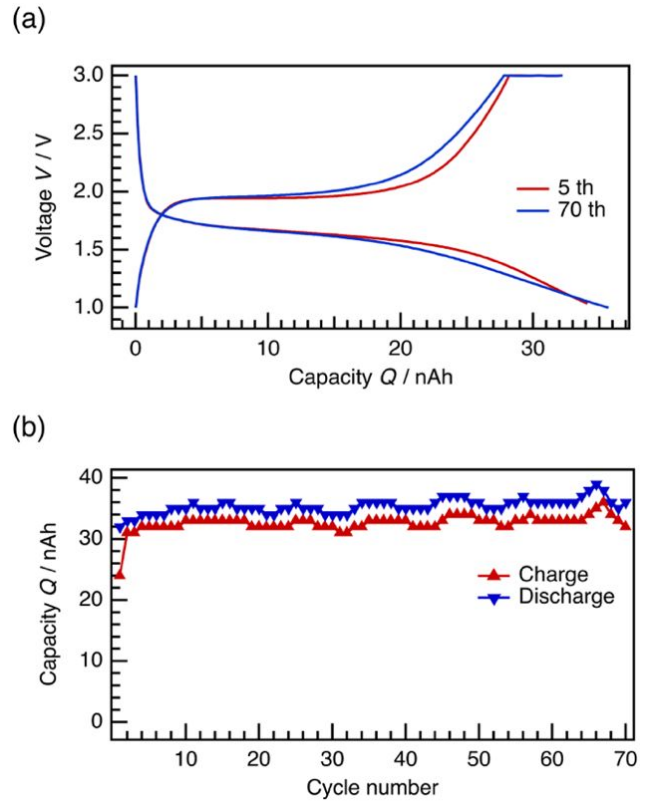

Fig. 2 (a) CC-CV charge/CC discharge curves. (b) capacity retention curves under dark. The CC charge/discharge currents are 0.1 C.

indeed absorb light transmitted through the $LaSrAlO_4$(001) substrate (Fig. S5). In assembling a thin-film ASSB, a layer of Li_3PO_4 solid electrolyte and a metallic Li anode were deposited atop the a-TiO_2:Nb/$CaRuO_3$/$LaSrAlO_4$(001) structure. Consequently, we concluded that the configuration of Li/Li_3PO_4/a-TiO_2:Nb/$CaRuO_3$/$LaSrAlO_4$(001) in the thin-film ASSB was suitable for investigating the photo-response of a-TiO_2:Nb when exposed to light irradiation from the $LaSrAlO_4$(001) side.

We confirmed the charge/discharge properties of Li/Li_3PO_4/a-TiO_2:Nb/$CaRuO_3$/$LaSrAlO_4$(001) under dark conditions before the measurements under light irradiation. Fig. 2 shows charge/discharge curves and capacity retentions under dark conditions. The charge and discharge were carried out with constant-current + constant-voltage (CC-CV) and constant-current (CC) modes, respectively. The charge/discharge rates in the CC modes were 0.1 C, and the voltages in the CV modes were 3.0 V. Due to Li^+-(de)intercalation from/into a-TiO_2:Nb, the plateau region was confirmed around 1.75 V of the voltage during charge/discharge. In addition, the charge/discharge reaction reversibly proceeded over 70 cycles. These results indicate that the Li/Li_3PO_4/a-TiO_2:Nb/$CaRuO_3$/$LaSrAlO_4$(001) structure operates reliably as a thin-film ASSB, even without light. Consequently, we have established that Li/Li_3PO4/a-TiO_2:Nb/$CaRuO_3$/$LaSrAlO_4$(001) is suitable for exploring the photo-response associated with Li^+-deintercalation.

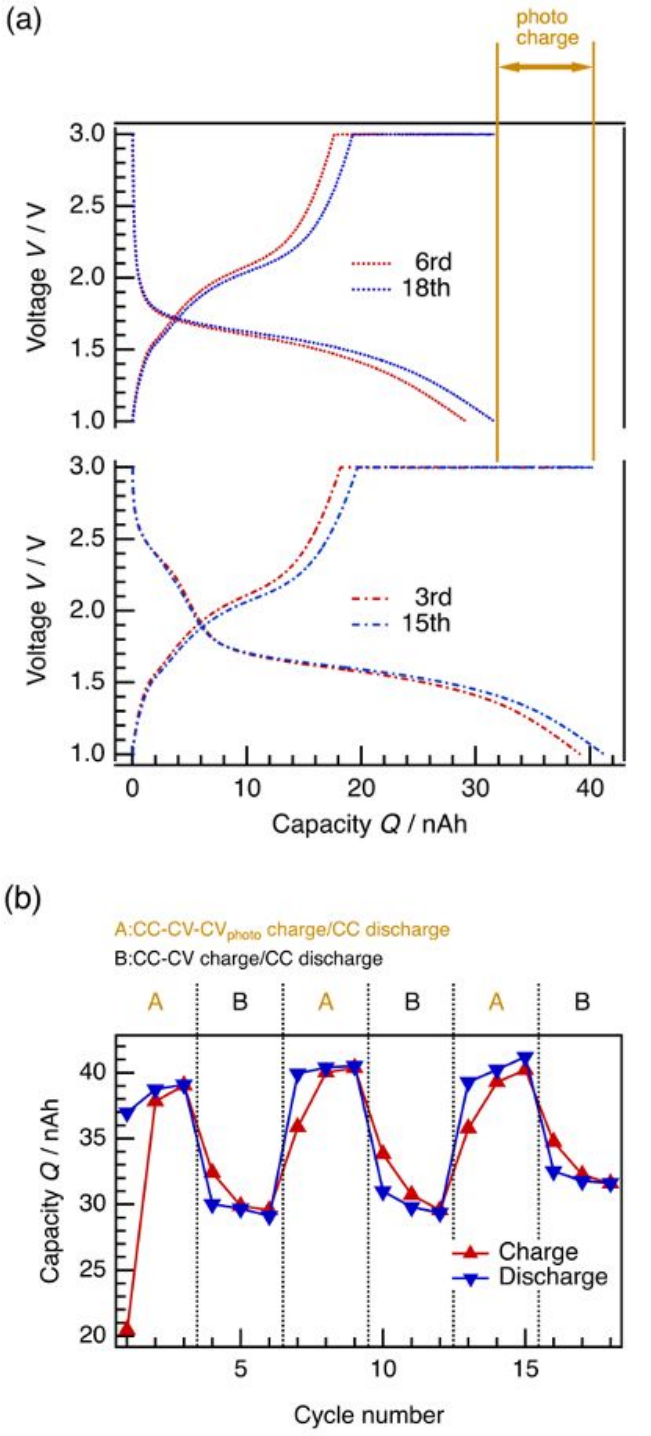

Fig. 3 (a) CC-CV-CVphoto charge/CC discharge curves. (b) capacity retention curves. The CC charge/discharge currents are 0.5 C.

Investigation of the photo-responsive Li^+-deintercalation from a-TiO_2:Nb cathode

The photo-response of the charge was initially investigated, as illustrated in Fig. 3. The charging was conducted under constant-current + constant-voltage + constant-voltage with light irradiation (CC-CV-CV_{photo}) modes. The light was only applied during CV_{photo} charging, which occurred for 1 h following 1 h of CV charging. In cases where CV_{photo} charging was omitted

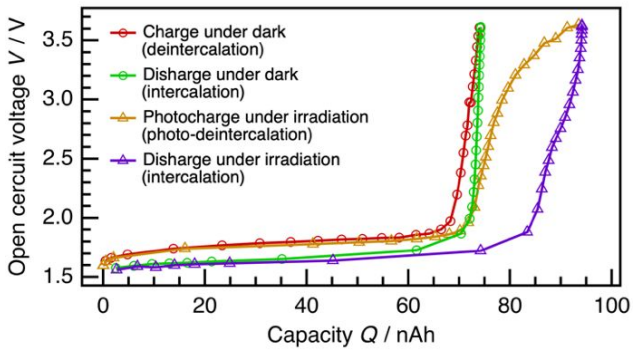

Fig. 4 Open circuit voltage (OCV) curves at CC-CV-OCV measurements.

(CC-CV charging), CV charging was carried out for 2 h. The charge capacities were significantly enhanced by light irradiation (Fig. 3a). The capacities obtained during CV_{photo} charging closely matched the discharge capacities following CV_{photo} charging. Moreover, the discharge capacities within the plateau region around 1.75 were also increased by light irradiation. Furthermore, these capacities were maintained over 9 cycles, even during CC-CV-CV_{photo} charging and subsequent discharge (Fig. 3b). These findings suggest that the charge reaction under light irradiation exhibits reversibility compared to the discharge reaction under dark conditions. Additionally, in the discharge curves following CC-CV-CV_{photo} charging, new discharge capacities were observed between 2.8 V and 1.9 V. These charge/discharge characteristics are consistent with those previously reported for polycrystalline a-TiO_2:Nb films in our prior study.[25] Consequently, the charge/discharge behaviour appears to be well-founded.

Charge properties under light irradiation were further investigated electrochemically. Fig. 4 depicts the open circuit voltage (OCV) curves under dark conditions and light irradiation. During these measurements, OCV values were recorded at various charge/discharge states, both in the absence of light and under light irradiation, during CC charge/discharge. Notably, the charge capacity under light irradiation displayed a similar trend between OCV values of 1.5 V and 2.5 V compared to conditions without light. However, the charge capacity slightly increased under dark conditions beyond 2.5 V. In contrast, the charge capacity began to exhibit further growth under light irradiation beyond 2.5~3.0 V of OCV, leading to an overall increase in the charge capacity. During discharge, the plateau region around 1.6 V was visibly broadened by light irradiation, indicating an increased amount of Li^+-deintercalation. The temperature of the sample exhibited minimal changes due to light irradiation (Fig. S6), suggesting that the increased Li^+-deintercalation was not a result of thermal effects but rather the outcome of photogenerated charge carriers. Therefore, the photo-responsive Li^+-deintercalation has been electrochemically verified.

Li^+-deintercalation was conducted using *operando* XRD, as depicted in Fig. 5. In these *operando* XRD measurements, the 004 peak of a-TiO_2:Nb was continuously monitored during charge/discharge cycles. Under dark conditions (Fig. 5(a,b)), the 004 peak gradually shifted to a higher L-value with increasing intensity as the charging process advanced. These results indicate that Li^+ was indeed deintercalated from a-Li_xTiO_2:Nb. Upon discharging, the 004 peak reverted to its original L-value and intensity, signifying the reversible (de)intercalation of Li^+ ions in the absence of light. Under light irradiation (Fig. 5(c,d)), the 004 peak similarly shifted to a higher L-value than its pristine state, resembling the shift observed under dark conditions. However, the presence of light enhanced the peak intensity during charging. Furthermore, the full width half maximum (FWHM) of the peak under light irradiation was narrower than that observed under dark conditions. These findings suggest that a-Li_xTiO_2:Nb at the charged state more closely resembled pure a-TiO_2:Nb under light irradiation compared to dark conditions. Consequently, Li^+ ions were observed to deintercalate more significantly from a-Li_xTiO_2:Nb under light irradiation than in the absence of light. After charging under light irradiation, the 004 peak reverted to its pristine state during discharging. This observation indicates that Li^+ ions, deintercalated in response to light, were reversibly intercalated back into a-TiO_2:Nb. Thus, we have successfully demonstrated the photo-responsive Li^+-deintercalation with reversible intercalation ability, confirmed directly through *operando* XRD.

Our previous report established that a-TiO_2:Nb responds to irradiated light at potentials higher than its flat band potential (E_{FB}) in the all-solid-state photoelectrochemical cell.[25] Therefore, we also investigated the dependency of photo-responsive Li^+-deintercalation on applied voltage. Fig. 6 presents CC-CV-CV_{photo} charge/CC discharge curves with various upper cut-off voltages. When the applied voltage was ≥ 2.5 V (≈ E_{FB}[25]), the charge capacity increased due to light irradiation. All the charge capacities that increased due to light irradiation were discharged reversibly. Furthermore, the plateau regions around 1.75 V, indicative of Li^+-(de)intercalation in a-TiO_2, expanded as the voltage increased. These results indicate that photo-responsive Li^+-deintercalation occurs at potentials higher than E_{FB} and depends on the applied voltage. However, the discharge capacities increased not only at 1.75 V but also between 2.9 V and 1.9 V. The crystal structure of a-TiO_2:Nb remained unchanged during the discharge at 2.9~1.9 V (as shown in Fig. 5d), indicating that Li^+-intercalation did not occur. Therefore, the increased discharge capacities at 2.9~1.9 V might be attributed to photogenerated holes trapped at the a-TiO_2:Nb/Li_3PO_4 interface due to the bending of the a-TiO_2:Nb VB toward negative potential. This explains why the capacities at 2.9~1.9 V increased with the potential more positive than E_{FB}.[41] This result suggests that non-intercalative materials could be used as electrodes for photo-rechargeable supercapacitors.

Fig. 7 illustrates the proposed mechanism of photo-charge and discharge using Li/Li_3PO_4/a-TiO_2:Nb/$CaRuO_3$/$LaSrAlO_4$(001) in the thin-film ASSB. When charging at < 2.5 V (≈ E_{FB}) (Fig. 7a), photoexcited electrons migrate to the a-TiO_2:Nb/Li_3PO_4 interface owing to the CBM bending toward positive potential or recombining with holes, which does not increase capacity. Conversely, when the potential of a-TiO_2:Nb was more positive than E_{FB} (Fig. 7b), the photoexcited electrons can migrate to the current collector owing to the CBM bend toward negative potential. Subsequently, photogenerated holes in the VB are

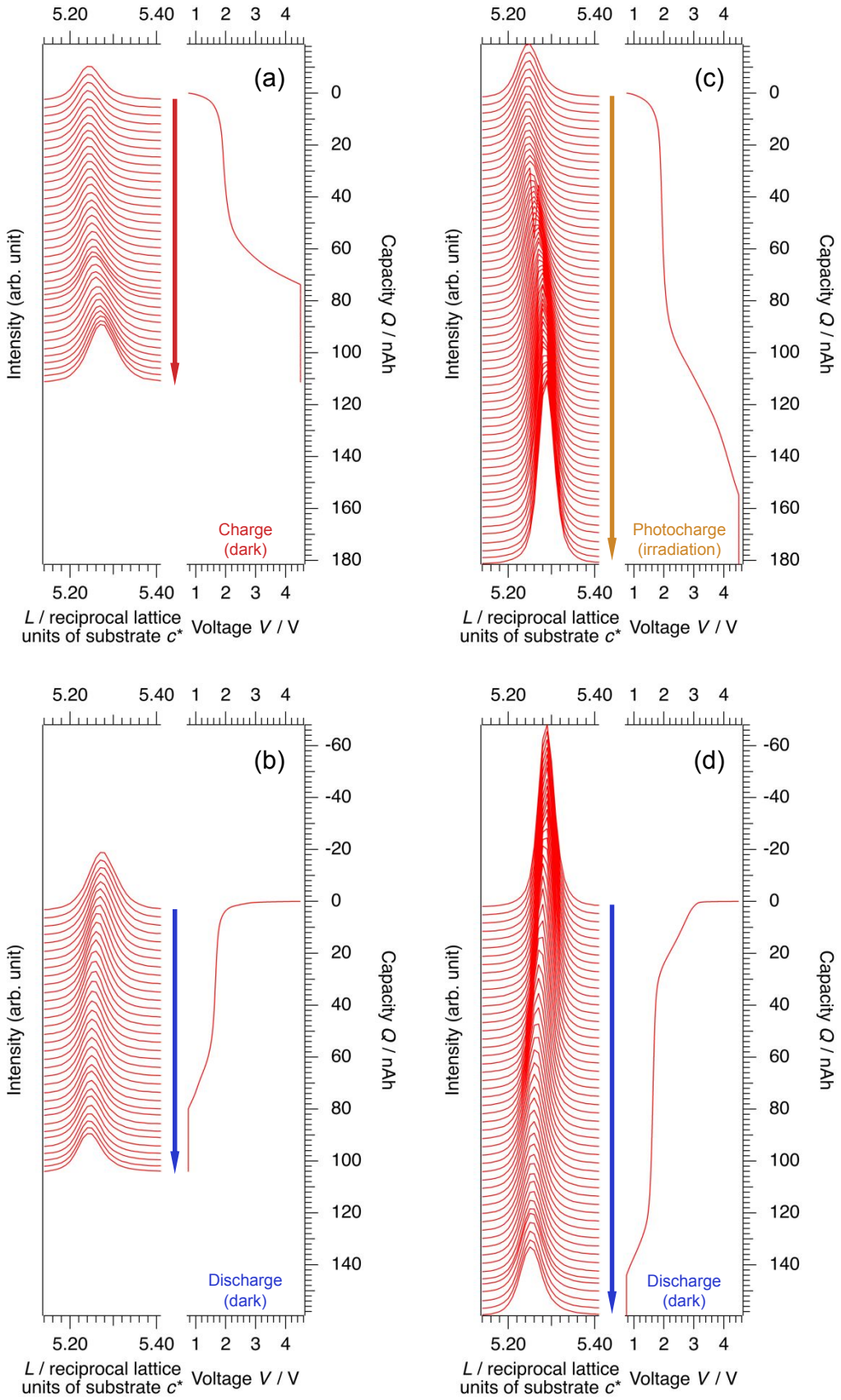

Fig. 5 *Operando* XRD patterns of Li_xTiO_2:Nb 004 peaks and (photo)charge/discharge curves (a) during CC-CV charge under dark, (b) during CC-CV discharge in dark, (c) during CC-CV photocharge under light irradiation, and (d) during CC-CV discharge in dark after photocharge.

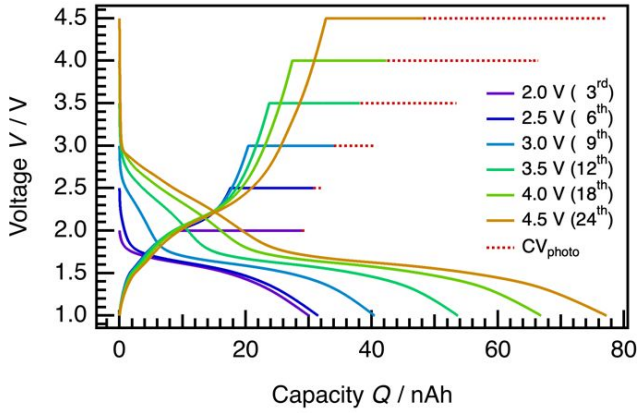

Fig. 6 CC-CV-CV_{photo} charge/CC discharge curves with different upper cut-off voltages. The CC charge/discharge currents are 0.5 C.

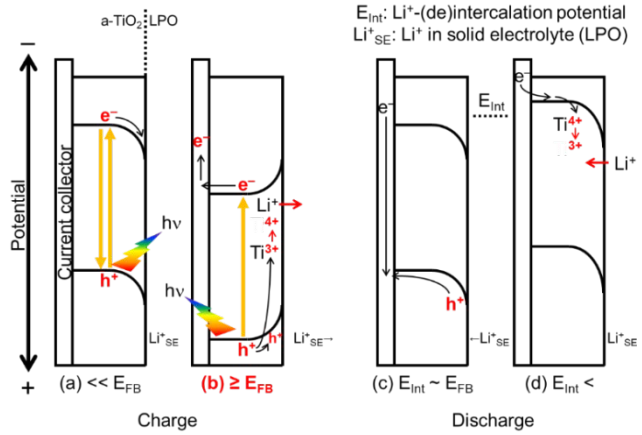

Fig. 7 Proposed mechanism of photo-charge and discharge.

situated at more positive levels than the fermi level (E_f), indicating that these holes possess a greater driving force for oxidation. Consequently, Li^+-deintercalation, corresponding to the oxidation of Ti(III) to Ti(IV), is accelerated by the photogenerated holes, increasing capacity. Furthermore, a portion of the photogenerated holes is stored in the depletion layer formed by the band bending at the a-TiO_2:Nb/Li_3PO_4 interface. As a result, certain Li ions in Li_3PO_4 migrate from the interface into the bulk, forming an electric double layer (capacitance). During discharge at 2.9~1.9 V, the holes stored at the a-TiO_2:Nb/Li_3PO_4 interface flow toward the current collector due to relieving the VBM bending toward negative potential. Starting from approximately 1.75 V, all the Li ions, which deintercalated with or without photo-assistance, are reversibly intercalated into a-TiO_2:Nb.

In the photo-recharge, there are 2 additional processes, which are absorption of incident light and separation of photogenerated carriers. These processes can be controlled by engineering a band structure of an electrode material. A band gap directly results in the number of absorbed photons. The photogenerated carriers are separated with depending on band bending. Moreover, external bias required for photo-charge depends a flat band potential of the electrode material. Ideally, if a battery is charged only by light irradiation without external bias, photoexcited electrons should be located at more negative potential than reaction potential of counter electrodes with keeping the band bending toward negative potential. From these points, a conduction band of an electrode with a narrow band gap should be located at a potential as negative as possible. In addition, suppressing the recombination between electrons and holes is important to improve performance of photo-rechargeable batteries. Introducing buffer layers and adjustment of band bending and gradient are useful method to control carrier separation in photoelectrodes.[42,43] Also in the field of the solar cell, field effect passivation is often utilized to suppress the recombination between electrons and holes.[44-47] Therefore, the photo-rechargeable battery would be also improved by introducing buffer/passivation layers and band engineering.

In summary, we have successfully elucidated both reversible Li^+-(de)intercalative and non-intercalative photo-recharge processes, which can be applied to photo-rechargeable batteries and supercapacitors for solar energy utilization. These insights into Li^+-(de)intercalative and non-intercalative photo-recharge were attained through an all-solid-state cell incorporating a stable solid electrolyte. Consequently, all-solid-state cells have the potential to significantly contribute to solar energy conversion and storage.

Conclusions

We have successfully elucidated the processes of Li^+-deintercalation and non-intercalative photo-charge using a-TiO_2:Nb/Li_3PO_4/Li in the thin-film ASSB and *operando* XRD. The amount of Li^+ ions deintercalated from a-TiO_2:Nb was increased by the light irradiation. The Li^+ ions deintercalated with the photo-assistance were reversibly intercalated again into a-TiO_2:Nb, implying that the photo-energy capacity could be used for discharge. The charge capacity under light irradiation was partially derived from the electric double layer at a-TiO_2:Nb/Li_3PO_4 interface comprising holes photogenerated in a-TiO_2:Nb and Li^+-vacancies in Li_3PO_4. This finding suggests the potential application of non-intercalative photoelectrodes in photo-rechargeable supercapacitors. Conversely, photo-(de)intercalative materials should be employed in the context of photo-rechargeable batteries. Utilizing the ASSB configuration with a stable solid electrolyte proved instrumental in elucidating the mechanisms underlying both Li^+-(de)intercalative and non-intercalative photo-recharge processes. Consequently, ASSBs hold significant promise in advancing the field of solar energy conversion and storage.

Author Contributions

M. Yoshimoto mainly conducted the experiments and wrote the original draft. K. Tamura measured *operando* XRD as a collaborative researcher. K. Watanabe supervised the project and mainly revised the original draft. K. Shimizu supported the

experiments. T. Kobayashi, H. Tsurita and Y. Horisawa investigated and developed experimental method of photo-rechargeable cells. R. Kanno and K. Suzuki supervised the project. M. Hirayama administrated and supervised the project.

Conflicts of interest

There are no conflicts to declare.

Acknowledgements

This work was supported by JSPS KAKENHI (Grant Numbers: JP16K05929, JP19H02808, JP19H05785, JP19H05793, JP22J11242 and JP22KJ1299), JST ACT-X (Grant Number JPMJAX22KK), JST SPRING (Grant Number JPMJSP2106), JST OPERA (Grant Number JPMJOP1862), and Leave a Nest Grant, Focus Systems Award, Japan. The synchrotron X-ray experiments were performed as projects approved by the Japan Synchrotron Radiation Research Institute (JASRI) (Proposal No. 2019A3635, 2020A3742, 2021A3742, 2021B1907, 2021B3738, 2022A3741, 2022B3741 and 2023A3741). We thank Dr. Tomoyuki Koganezawa at the JASRI for his assistance with *operando* XRD. The authors would like to thank Mr. S. Oomori, Mr. S. Murata, and Mr. T. Sugihara at Design and Manufacturing Division, Open Facility Center, Tokyo Institute of Technology, for preparing the sample.

References

1 B. A. Pinaud, J. D. Benck, L. C. Seitz, A. J. Forman, Z. Chen, T. G. Deutsch, B. D. James, K. N. Baum, G. N. Baum, S. Ardo, H. Wang, E. Miller and T. F. Jaramillo, *Energy Environ. Sci.*, 2013, **6**, 1983–2002.
2 D. M. Fabian, S. Hu, N. Singh, F. A. Houle, T. Hisatomi, K. Domen, F. E. Osterloh and S. Ardo, *Energy Environ. Sci.*, 2015, **8**, 2825–2850.
3 J. W. Ager, M. R. Shaner, K. A. Walczak, I. D. Sharp and S. Ardo, *Energy Environ. Sci.*, 2015, **8**, 2811–2824.
4 T. Setoyama, T. Takewaki, K. Domen and T. Tatsumi, *Faraday Discuss.*, 2017, **198**, 509–527.
5 S. Ardo, D. Fernandez Rivas, M. A. Modestino, V. Schulze Greiving, F. F. Abdi, E. Alarcon Llado, V. Artero, K. Ayers, C. Battaglia, J. P. Becker, D. Bederak, A. Berger, F. Buda, E. Chinello, B. Dam, V. Di Palma, T. Edvinsson, K. Fujii, H. Gardeniers, H. Geerlings, S. M. Hashemi, S. Haussener, F. Houle, J. Huskens, B. D. James, K. Konrad, A. Kudo, P. P. Kunturu, D. Lohse, B. Mei, E. L. Miller, G. F. Moore, J. Muller, K. L. Orchard, T. E. Rosser, F. H. Saadi, J. W. Schüttauf, B. Seger, S. W. Sheehan, W. A. Smith, J. Spurgeon, M. H. Tang, R. Van De Krol, P. C. K. Vesborg and P. Westerik, *Energy Environ. Sci.*, 2018, **11**, 2768–2783.
6 R. ABE, K. SAYAMA, K. DOMEN and H. ARAKAWA, *Chem. Phys. Lett.*, 2001, **344**, 339–344.
7 R. Abe, *J. Photochem. Photobiol. C Photochem. Rev.*, 2010, **11**, 179–209.
8 R. Abe, *Bull. Chem. Soc. Jpn.*, 2011, **84**, 1000–1030.
9 T. Miyasaka and T. N. Murakami, *Appl. Phys. Lett.*, 2004, **85**, 3932–3934.
10 H. Usui, K. Koseki, T. Tamura, Y. Domi and H. Sakaguchi, *Mater. Lett.*, 2017, **186**, 338–340.
11 H. Nagai and H. Segawa, *Chem. Commun.*, 2004, **4**, 974–975.
12 H. Tributsch, *Faraday Discuss. Chem. Soc.*, 1980, **70**, 189–205.
13 G. Betz and H. Tributsch, *Prog. Solid State Chem.*, 1985, **16**, 195–290.
14 X. Zou, N. Maesako, T. Nomiyama, Y. Horie and T. Miyazaki, *Sol. Energy Mater. Sol. Cells*, 2000, **62**, 133–142.
15 X. Zou, T. Nagao, O. Miyamoto, T. Nomiyama, Y. Horie and T. Miyazaki, *Japanese J. Appl. Physics, Part 1 Regul. Pap. Short Notes Rev. Pap.*, 2004, **43**, 7707–7713.
16 T. Nomiyama, H. Takeuchi, K. Kawazoe, Y. Horie and T. Miyazaki, *Japanese J. Appl. Physics, Part 1 Regul. Pap. Short Notes Rev. Pap.*, 2005, **44**, 5219–5224.
17 H. Usui, O. Miyamoto, T. Nomiyama, Y. Horie and T. Miyazaki, *Sol. Energy Mater. Sol. Cells*, 2005, **86**, 123–134.
18 O. Nguyen, E. Courtin, F. Sauvage, N. Krins, C. Sanchez and C. Laberty-Robert, *J. Mater. Chem. A*, 2017, **5**, 5927–5933.
19 C. Andriamiadamanana, I. Sagaidak, G. Bouteau, C. Davoisne, C. Laberty-Robert and F. Sauvage, *Adv. Sustain. Syst.*, 2018, **2**, 1700166.
20 M. Nagasu and N. Koshida, *Appl. Phys. Lett.*, 1990, **57**, 1324–1325.
21 Y. Zhu, X. He and Y. Mo, *ACS Appl. Mater. Interfaces*, 2015, **7**, 23685–23693.
22 Y. Zhu, X. He and Y. Mo, *J. Mater. Chem. A*, 2016, **4**, 3253–3266.
23 W. D. Richards, L. J. Miara, Y. Wang, J. C. Kim and G. Ceder, *Chem. Mater.*, 2016, **28**, 266–273.
24 J. D. LaCoste, A. Zakutayev and L. Fei, *J. Phys. Chem. C*, 2021, **125**, 3651–3667.
25 K. Watanabe, Y. Horisawa, M. Yoshimoto, K. Tamura, K. Suzuki, R. Kanno and M. Hirayama, *Nano Lett.*, in press.
26 X. Wei, X. Wang, Q. An, C. Han and L. Mai, *Small Methods*, 2017, **1**, 1–13.
27 K. Sakamoto, M. Hirayama, H. Konishi, N. Sonoyama, N. Dupré, D. Guyomard, K. Tamura, J. Mizuki and R. Kanno, *Phys. Chem. Chem. Phys.*, 2010, **12**, 3815.
28 M. Hirayama, H. Ido, K. Kim, W. Cho, K. Tamura, J. Mizuki and R. Kanno, *J. Am. Chem. Soc.*, 2010, **132**, 15268–15276.
29 M. Hirayama, *Electrochemistry*, 2015, **83**, 701–706.
30 K. Hikima, Y. Hinuma, K. Shimizu, K. Suzuki, S. Taminato, M. Hirayama, T. Masuda, K. Tamura and R. Kanno, *ACS Appl. Mater. Interfaces*, 2021, **13**, 7650–7663.
31 C. Cavallo, G. Calcagno, R. P. de Carvalho, M. Sadd, B. Gonano, C. M. Araujo, A. E.C. Palmqvist, and A. Matic, *ACS Appl. Energy Mater.*, 2021, **4**, 215–225.
32 H. Kato, K. Asakura, and A. Kudo, *J. Am. Chem. Soc.*, 2003, **125**, 3082-308.
33 Y. Ham, T. Hisatomi, Y. Goto, Y. Moriya, Y. Sakata, A. Yamakata, J. Kubotad and K. Domen, *J. Mater. Chem. A*, 2016, **4**, 3027–3033.
34 Y. Sakata, T. Hayashi, R. Yasunaga, N. Yanaga and H. Imamura, *Chem. Commun.*, 2015, **51**, 12935—12938.
35 T. Takata, J. Jiang, Y. Sakata, M. Nakabayashi, N. Shibata, V. Nandal, K. Seki, T. Hisatomi and K. Domen, *Nature*, 2020, **581**, 411—414.
36 L. G. Parratt, *Phys. Rev.*, 1954, **95**, 359–369.
37 Q. Jia, K. Iwashina and A. Kudo, *Proc. Natl. Acad. Sci. U. S. A.*, 2012, **109**, 11564–11569.
38 Y. Kawase, T. Higashi, M. Katayama, K. Domen and K. Takanabe, *ACS Appl. Mater. Interfaces*, 2021, **13**, 16317–16325.
39 A. Iwase, S. Ikeda and A. Kudo, *Chem. Lett.*, 2017, **46**, 651–654.
40 T. Higashi, H. Nishiyama, Y. Suzuki, Y. Sasaki, T. Hisatomi, M. Katayama, T. Minegishi, K. Seki, T. Yamada and K. Domen, *Angew. Chemie - Int. Ed.*, 2019, **58**, 2300–2304.
41 H. Usui, S. Suzuki, Y. Domi and H. Sakaguchi, *Mater. Today Energy*, 2018, **9**, 229–234.
42 Y. Goto, T. Minegishi, Y. Kageshima, T. Higashi, H. Kaneko, Y. Kuang, M. Nakabayashi, N. Shibata, H. Ishihara, T. Hayashi, A.

Kudo, T. Yamada and K. Domen, *J. Mater. Chem. A*, 2017, **5**, 21242–21248.
43 T. Minegishi, *Appl. Phys. Lett.*, 2021, **119**, 123905.
44 A. G. Aberle, S. Glut-q and W. Warta, *J. Appl. Phys.*, 1992, **71**, 4422–4431.
45 A. G. Aberle, *Sol. Energy Mater Sol. Cells .*, 2001, **65**, 239–248.
46 B. Chaudhary, A. Kulkarni, A. K. Jena, M. Ikegami, Y. Udagawa, H. Kunugita, K. Ema and T. Miyasaka, *ChemSusChem*, 2017, **10**,2473 –2479.
47 Z. Guo, S. Zhao, N. Shibayama, A. K. Jena, I. Takei and T. Miyasaka, *Adv. Funct. Mater.*, 2022, **32**, 2207554.